Articles

Contribution from the Department of Chemistry,
Texas A&M University, College Station, Texas 77843-3256

Single-Crystal Structure of Ta_3S_2. Structure and Bonding in Ta_6S_n (n = 1, 3, 4, 5?) Pentagonal-Antiprismatic Chain Compounds

Sung-Jin Kim, K. S. Nanjundaswamy, and Timothy Hughbanks*

Received July 12, 1990

The single-crystal structure of the new binary sulfide Ta_3S_2 is reported and discussed in light of the known structures of Ta_6S, Ta_2S, and the as yet unrealized one-dimensional Ta_6S_5 chain. Ta_3S_2 crystallizes in the orthorhombic space group *Abm*2 (No. 39) with lattice parameters a = 7.4783 (6) Å, b = 17.222 (1) Å, c = 5.6051 (4) Å, V = 721.88 (9) Å^3, and Z = 8. While the structure is in accord with that reported for Ta_3S_{2-x} ($0.2 \le x \le 0.28$) by Wada and Onoda using X-ray Rietveld analysis, we find Ta_3S_2 to be a stoichiometric compound with no appreciable phase width up to 1300 °C. Band structure calculations reveal that as sulfur content in the Ta_6S_n (n = 1, 3, 4, 5) series increases, the Ta–Ta bonding remains optimal, as judged by the behavior of COOP curves for the metal–metal bonding in these compounds. While Ta_2S should be an electrical conductor, Ta_3S_2 should be a poor conductor or semimetallic and Ta_6S_5 chains are predicted to be semiconducting.

Introduction

The insertion of sulfur into tantalum wreaks a tremendous change upon the metal's body-centered cubic structure. Franzen and Smeggil long ago discovered that Ta-centered pentagonal-antiprismatic chains, $^1_\infty[Ta_5Ta]$, occur in the Ta-rich compounds Ta_2S (=Ta_6S_3) and Ta_6S.[1,2] A triclinic modification of Ta_6S has also been uncovered.[3] Recently, Wada and Onoda reported a phase with the composition $Ta_3S_{1.8}$ and, using Rietveld analysis of X-ray powder data, determined that its structure incorporates $^1_\infty[Ta_5Ta]$ units linked in a way quite similar to Ta_2S.[4] New tantalum chalcogenides have been uncovered in other laboratories. There is a strong structural similarity of the 5-fold symmetry Ta-centered chains discussed herein and the 4-fold symmetric chains found in the recently discovered Ta_4ZTe_4 (Z = Al, Si, Cr–Ni) series of compounds.[5,6] The remarkable new compound Ta_2Se has a layer structure quite simply related to the bulk bcc Ta; four square-net Ta layers ([100] planes) are inserted between two square-net Se layers.[7] These thick sandwiches are then stacked with van der Waals gaps between them. Tricapped trigonal-prismatic Ta chains are centered with Fe, Co, or Ni (=M) atoms in $Ta_9S_6M_2$ and $Ta_{11}Se_8M_2$ ternaries.[8-10]

In the present paper we report the single-crystal structure of Ta_3S_2 (=Ta_6S_4) and present a study of the electronic structure of the remarkable Ta_6S_n series. A one-dimensional building block $^1_\infty[Ta_5TaS_5]$ is explored as a potential member of this series and is found to be an attractive synthetic target.

Experimental Procedures

Syntheses. Our investigations grew out of attempts to find lower temperature routes to metal-rich tantalum sulfides. $Ta_9S_6Fe_2$ crystals can be grown at 1000 °C in vapor-phase transport reactions using stoichiometric ratios of TaS_2, Ta, and Fe metal powders with a trace of $TaBr_5$ used as a transport reagent. TaS_2 was prepared previously by reaction of the elements in a sealed silica vessel at 500 °C. The transport reactions were carried out in sealed Ta capsules that were in turn encased in evacuated silica tubes. The high surface area of the Ta powder and the stability of the product reduce the extent of reaction of sulfur with the walls of the Ta capsule, though some embrittlement of the capsule was observed. Despite the obvious inability to completely control Ta composition under these conditions, good crops of needle-shaped $Ta_9S_6Fe_2$ crystals can be grown. Ta_3S_2 single crystals were originally grown in vapor-phase transport reactions designed for the synthesis of new $Ta_9S_6Ru_2$ analogues of the known $Ta_9S_6M_2$ (M = Fe, Co, Ni) compounds.[8,9] (No ternary Ta–S–Ru products have been uncovered to date.) Typically, reactions are run at 1000 °C for 2 weeks with $TaBr_5$ used as a transport reagent. Yields of Ta_3S_2 are erratic when the transport method is used due to involvement of the Ta tubes in the reactions. Direct reaction using pressed pellets is preferable if bulk quantities are desired. Attempts to use silica as a container inevitably lead to attack of silica and formation of tantalum silicide, Ta_2Si.[11]

Pressed-pellet reactions to prepare binary tantalum sulfides were carried out in a manner intended to follow the procedure used by Wada and Onoda,[4] except that welded tantalum tubes were used instead of alumina crucibles as the containers. A series of pellets using Ta powder and TaS_2 in the compositions Ta_xS_2 (x = 2.4, 2.75, 3.0, 3.25) were heated in separate tubes over a period of 24 h at 1000 °C and then for 5 h at 1300 °C. The pellets were then removed, reground and repelletized, then heated as before for 5 h at 1300 °C, and then air-quenched. In each case the Ta tubes were welded under an argon atmosphere and sealed in a silica jacket under an argon atmosphere at about 200-mm pressure (at room temperature). A moderate embrittlement of the Ta tubes was generally observed, indicating some sulfur loss from the pellets to the surrounding container. Sulfur loss can be reduced by wrapping the pellets in molbydenum foil before putting them in the Ta tubes. The silica jackets showed no sign of reaction, and devitrification was minimal for well-cleaned ampules.

Combustion analyses were carried out for pellet reaction products by air oxidation of the samples at 800 °C and by weighing the white products as Ta_2O_5. Electron microprobe analyses were performed by using a JSM T330A instrument on products of the single-crystal vapor-phase reactions carried out in Ta tubes. For crystals of sufficient size for accurate analysis, Ta_6S was usually observed—undoubtedly the result of involvement of the walls in the reaction.

X-ray Studies. A black needle-shaped crystal of Ta_3S_2 having approximate dimensions of 0.20 × 0.075 × 0.50 mm was mounted on a glass fiber. All measurements were made on a Rigaku AFC5R diffractometer with graphite-monochromated Mo Kα radiation and a 12-kW rotating anode generator. Data collection and structure refinement were performed with the aid of the TEXSAN crystallographic software package.[12a] Cell constants and an orientation matrix for data collection,

* To whom correspondence should be addressed.

(1) Franzen, H. F.; Smeggil, J. G. *Acta Crystallogr., Sect. B* **1969**, *25*, 1736.
(2) Franzen, H. F.; Smeggil, J. G. *Acta Crystallogr., Sect. B* **1970**, *26*, 125.
(3) Harbrecht, B. *J. Less-Common Met.* **1988**, *138*, 225.
(4) Wada, H.; Onoda, M. *Mater. Res. Bull.* **1989**, *24*, 191.
(5) Badding, M. E.; Li, J.; DiSalvo, F. J. Paper presented at the 199th National Meeting of the American Chemical Society, Boston, MA, 1990.
(6) DiSalvo, F. J. *Science* **1990**, *247*, 649.
(7) Harbrecht, B. *Angew. Chem., Int. Ed. Engl.* **1989**, *28*, 1660.
(8) Harbrecht, B.; Franzen, H. F. *J. Less-Common Met.* **1985**, *113*, 349.
(9) Harbrecht, B. *J. Less-Common Met.* **1986**, *124*, 125.
(10) Harbrecht, B. *J. Less-Common Met.* **1988**, *141*, 59.
(11) Schäfer, H. *Chemical Transport Reactions*; Academic Press: New York, 1964.

0020-1669/91/1330-0159$02.50/0

Table I. Crystallographic Data for Ta_3S_2

chem formula	Ta_3S_2
a, Å	7.480 (2)
b, Å	17.232 (3)
c, Å	5.608 (1)
V, Å^3	722.8 (3)
Z	8
fw	606.976
space group	*Abm*2 (No. 39)
T, °C	21
λ, Å	0.71073
abs coeff (μ) (Mo Kα), cm^{-1}	904.34
transm coeff range	0.86–1.0
cryst dimens, mm	0.20 × 0.075 × 0.50
2θ(max), deg	60
no. of reflns	
measd ($\pm h,\pm k,\pm l$)	4202
unique	1157 (R_{int} = 4.7%)
unique obsd ($I > 3\sigma(I)$)	883
no. of variables	48
secondary ext coeff (10^{-9})	4.1
R,[a] %; R_w,[b] %	2.7; 3.1
goodness of fit indicator	1.30
max (min) peaks in final diff map, e/Å^3	3.11 (−2.78)

[a] $R_w = \sum(|F_o| - |F_c|)/\sum|F_o|$. [b] $[\sum w(|F_o| - |F_c|)^2]^{1/2}$, $w = 4F_o^2/\sigma^2(F_o^2)$.

obtained from a least-squares refinement using setting angles of three carefully centered relfections in the range 47.3° < 2θ < 48.1°, corresponded to an orthorhombic unit cell with dimensions a = 7.480 (2) Å, b = 17.232 (3) Å, c = 5.608 (1) Å, and V = 722.8 (3) Å^3. (The Guinier powder diffraction parameters are generally more accurate: a = 7.4783 (6) Å, b = 17.222 (1) Å, c = 5.6051 (4) Å, V = 721.88 (9) Å^3.) On the basis of the observed systematic absences (hkl: $k + l \neq 2n$; $0kl$: $k \neq 2n$), packing considerations, a statistical analysis of the intensity distribution, and the successful refinement of the structure, the space group was determined to be *Abm*2 (No. 39). Data were collected at room temperature by using ω–2θ for reflections with $2\theta < 60°$. Scans of (1.31 + tan θ)° were made at a speed of 4.0°/min in ω. The weak reflections ($I < 10\sigma(I)$) were rescanned (up to two rescans), and counts were accumulated to ensure good counting statistics. Intensities for three check reflections did not decay throughout data collection. Data were collected for a full sphere ($\pm h,\pm k,\pm l$) to gain full advantage of data averaging. An empirical absorption correction was applied on the basis of Ψ-scans for several reflections. The absorption coefficient is large ($\mu_{Mo K\alpha}$ = 904.34 cm^{-1}), and Friedel pairs were *not* averaged for this acentric space group.

Tantalum atoms were located by using direct methods.[12b,c] Sulfur positions were determined by examination of electron density difference maps and by applying constraints imposed by avoiding unrealistically short S–S contacts. The known Ta_2S structure was used in devising structural models for refinement.[1] Data collection and refinement parameters are given in Table I. Neutral-atom scattering factors were taken from Cromer and Waber.[13a] Anomalous dispersion effects were included in the F_c computation,[13b] real and imaginary parts were taken from Cromer.[13c] A secondary extinction correction was applied. Since sulfur vacancies had been reported in earlier work, we attempted to refine the structure with variable sulfur occupancies. When neither of the sulfur atom occupancies departed significantly from unity, they were fixed at unity. Tantalum scattering naturally dominates the intensity data, and the determination of sulfur stoichiometry using this method is problematic at best.

Results and Discussion

The Ta_3S_2 Structure. As we mentioned in the introduction, Wada and Onoda described $Ta_3S_{1.8}$ as a substoichiometric compound with the "Ta_3S_2" structure, elucidated by use of Rietveld analysis of X-ray powder data.[4] The single-crystal results reported here are in correspondence with the powder structure and are best discussed in comparison with the closely related Ta_2S structure. Both Ta_3S_2 and Ta_2S may be thought of as built from condensed Ta_6S_5 chains, to form a two-dimensional Ta–Ta bonded network in the first case and a three-dimensional network in the second. Fully intact Ta_6S_5 chains have not yet been observed as distinct structural units in any compound, but we introduce this system in Figure 1 as both a device for discussing these structures and in anticipation of our treatment of bonding below.

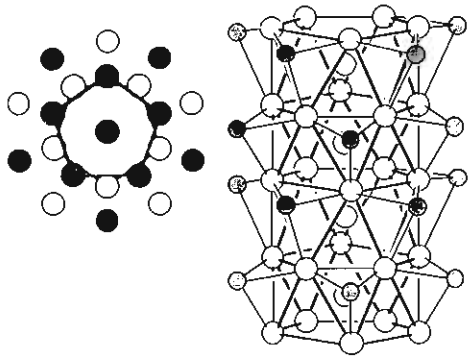

Figure 1. The Ta_6S_5 chain, a building block for Ta_2S and Ta_3S_2. The chain is viewed projected on the 5-fold axis at the upper left where the extent of shading is meant to indicate increasing heights of the atoms within one repeat unit. In the projection, only Ta–Ta bonds involving the tantalums in the pentagonal antiprism are shown. In the vertical view at right, sulfurs are stippled and sulfur atoms at the back have been omitted for clarity.

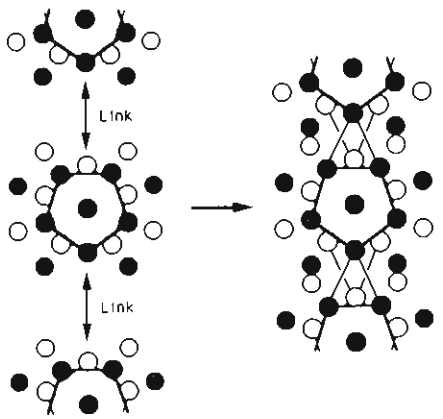

Figure 2. The linkage step for the construction of Ta_3S_2 layers. A sulfur atom has been removed from each layer in the Ta_6S_5 chains, and these chains are shown at left in the figure. All that remains is the coupling of these chains to form layers via the formation of interchain Ta–Ta bonds as shown. The "heights" of atoms are indicated by increased shading of atoms, as in Figure 1.

In the Ta_6S_5 chain, tantalum atoms are bound together in a chain of fused, centered pentagonal antiprisms. In an alternative description, the chains are built up by stacking Ta_5 pentagons in a staggered fashion with the addition of tantalum atoms to the center of the pentagonal antiprisms so generated. Thus, the centering metal atoms are in a somewhat compressed icosahedral environment. In the known binary tantalum sulfides the interlayer spacing between pentagons is in the range 2.62–2.80 Å (2.64 Å in monoclinic Ta_6S,[2] 2.62 Å in triclinic Ta_6S,[3] 2.79 Å in Ta_2S,[1] 2.80 Å in Ta_3S_2). Sulfur surrounds the $^1_\infty[Ta_5Ta]$ chain so as to cap alternant exposed triangular faces. To construct Ta_3S_2 from these Ta_6S_5 chains, a sulfur is removed from each S_5 layer, each taken from the opposite sides of adjacent layers. In the Ta_5 rings, this leaves three tantalum centers with only two sulfur atom neighbors, while two tantalum atoms remain coordinated by sulfur, as in the Ta_6S_5 chain. As depicted in Figure 2, these sulfur-deficient chains may then be linked by formation of interchain Ta–Ta bonds with the result that two-dimensional metal–metal bonded layers are formed. Figure 3 shows these layers in a vertical view,

(12) (a) *TEXSAN–TEXRAY Structure Analysis Package*; Molecular Structure Corp.: Woodlands, TX, 1985. (b) Gilmore, C. J. *J. Appl. Crystallogr.* **1984**, *17*, 42. (c) Beurskens, P. T. DIRDIF: Direct methods for Difference Structures. Technical Report 1984/1; Crystallography Laboratory: Toernooiveld, 6525 Ed Nijmegen, The Netherlands.

(13) (a) Cromer, D. T.; Waber, J. T. *International Tables for X-ray Crystallography*; The Kynoch Press: Birmingham, England, 1974; Vol. IV, Table 2.2 A. (b) Ibers, J. A.; Hamilton, W. C. *Acta Crystallogr.* **1964**, *17*, 781. (c) Cromer, D. T. *International Tables for X-ray Crystallography*; The Kynoch Press: Birmingham, England, 1974; Vol. IV, Table 2.3.1.

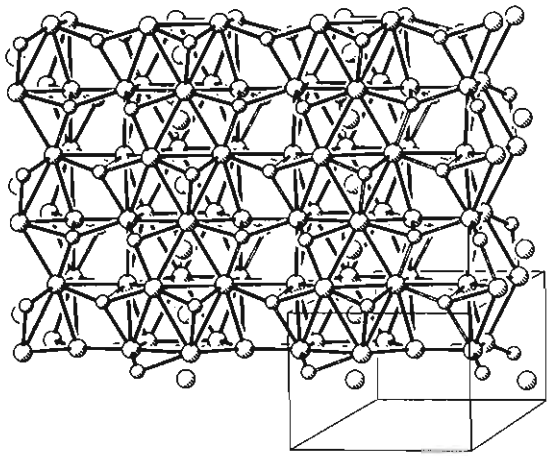

Figure 3. "Vertical" view of the interchain linkage for the layers in Ta_3S_2. Note that in addition to the formation of Ta–Ta bonds between chains, Ta–S bonds are formed. Essentially the same layers may be identified in Ta_2S. In Ta_3S_2 this is a (010) projection, and in Ta_2S it would be a (110) projection.

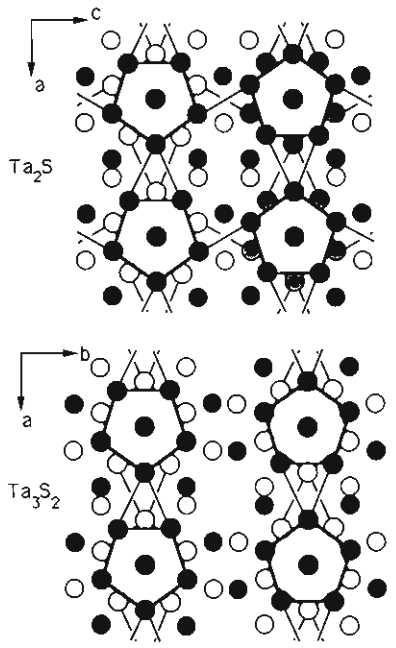

Figure 4. Ta_2S and Ta_3S_2 structures, projected on planes normal to the pentagonal antiprismatic chains ((010) for Ta_2S, (001) for Ta_3S_2). Shading of atoms is intended to indicate the heights of atoms in the direction normal to the plane of projection (y values for Ta_2S, z values for Ta_3S_2; these values increase with the intensity of shading). Only Ta–Ta bonds within and between the pentagonal antiprisms are indicated.

where one may see that interchain Ta–S bonds are formed as well. The net result is that sulfurs are four-coordinate, and sulfurs that cap triangular faces on one chain fill an open coordination site for tantalum atoms on adjacent chains. In Figure 4, these layers are seen to extend in the *ac* planes for Ta_3S_2 and in the *ab* planes for Ta_2S. These two-dimensional layers link together in Ta_3S_2 so that the remaining open coordination site at two tantalums in each Ta_5 ring is filled by sulfurs in the adjacent layers. Adjacent layers in Ta_3S_2 are held together solely by interlayer Ta–S bonds. Looking back to Figure 3, it is the three-coordinate sulfurs that cap triangular faces and do *not* participate in binding the chains together *within* the layer that are used to form interlayer Ta–S bonds. Thus, in the full structure the sulfurs are all ultimately four-coordinate.

For Ta_2S the situation with respect to interlayer binding is different. The layers are *fused* so that sulfurs are shared between chains in adjacent layers. This brings the tantalum atoms in adjacent layers closer together, and Ta–Ta bonds now extend between the layers to complete the formation of a fully three-dimensional metal–metal bonded network in Ta_2S. In the projection shown in Figure 4 it may appear that one may obtain Ta_3S_2 from Ta_2S by the insertion of an additional layer of sulfurs into the latter. In fact, more careful study of the structure shows that every other layer of linked pentagonal-antiprismatic chains in Ta_2S has sulfurs capping the second set of alternant triangular tantalum faces in the chain. (Refer back to Figure 1 and move the sulfurs from the triangular faces where they are bound to the faces that are vacant—then construct the layer as indicated in Figures 2 and 3.)

Table II. Positional Parameters for Ta_3S_2

	x	y	z	B(eq), Å^2
Ta1	0.71896 (8)	0.16619 (3)	0	0.32 (2)
Ta2	0.10455 (7)	0.10730 (3)	0.9938 (3)	0.31 (2)
Ta3	0.6551 (1)	1/4	0.4794 (3)	0.35 (3)
Ta4	0.9942 (3)	1/4	0.7448 (4)	0.28 (3)
S1	0.8270 (6)	0.0398 (2)	0.8683 (8)	0.6 (1)
S2	0.5843 (5)	0.1154 (3)	0.3711 (8)	0.6 (1)

Table III. Important Distances in Ta_3S_2

Ta4–Ta1(×2)	2.893 (2)	Ta2–Ta1(×1)[a]	3.058 (1)
Ta4–Ta1(×2)	2.928 (2)	Ta2–Ta2(×2)	3.2105 (7)
Ta4–Ta2(×2)	2.946 (1)		
Ta4–Ta2(×2)	2.928 (1)	Ta1–Ta1(×1)[a]	2.888 (1)
Ta4–Ta3(×1)	2.941 (2)		
Ta4–Ta3(×1)	2.934 (2)	S1–Ta1(×1)	2.437 (4)
Ta4–Ta4(×2)	2.8052 (6)	S1–Ta2(×1)	2.455 (5)
		S1–Ta2(×1)	2.481 (5)
Ta3–Ta1(×2)	3.292 (2)	S1–Ta2(×1)[c]	2.680 (4)
Ta3–Ta1(×2)	3.089 (2)		
Ta3–Ta1(×2)[b]	3.151 (1)	S2–Ta1(×1)	2.472 (5)
Ta3–Ta2(×2)[a]	3.0471 (9)	S2–Ta2(×1)	2.431 (4)
		S2–Ta3(×1)	2.455 (5)
Ta2–Ta1(×1)	3.291 (2)	S2–Ta2(×1)[d]	2.537 (4)
Ta2–Ta1(×1)	3.231 (2)		

[a] Distances within a Ta_5 pentagon. [b] Ta–Ta distance between chains within a layer. [c] Ta–S distance between layers. [d] Ta–S distance between chains within a layer.

We now consider some details of the Ta_3S_2 structure. Refined positional parameters are listed in Table II; anisotropic thermal parameters for all atoms were refined and revealed nothing unusual. The latter parameters and structure factor data are available as supplementary material. Some important interatomic distances are given in Table III. Naturally, the Ta–Ta bonding dominates the structure of Ta_3S_2. Judging by the distances, among the strongest of these bonds are those involving the icosahedral tantalums that center the pentagonal-antiprismatic chains. The average distance from the centering tantalums to their neighbors is 2.91 Å, which is just 0.02 Å shorter than what one calculates by using Pauling's bond order relation[14a] and a Ta–Ta single-bond distance of 2.71.[14b] Relatively short Ta–Ta distances are observed for the contacts within the Ta_5 pentagons (average 3.02 Å); all of these distances are shorter than any found between pentagons. Attempts to discover further systematics in metal–metal distances do not appear to be fruitful. In particular, it is interesting to note that an attempt to link average distances to coordination numbers is useless, since every tantalum is 12-coordinate if one counts both sulfur and tantalum neighbors.

Distances from sulfur to tantalum indicate that the sulfurs are bound more strongly to the triangular faces which they "cap" than they are to metals in other chains. The interlayer Ta–S distnace of 2.68 Å is particularly long and suggests that bonding between layers is somewhat weaker than within them. This rather long interlayer Ta–S contact is dictated by steric crowding between sulfurs across the interlayer boundary, where very short 2.93-Å S–S contacts are found (see **1**). This contact is considerably

(14) (a) Pauling, L. *The Nature of the Chemical Bond*, 3rd ed.; Cornell University Press: Ithaca, New York, 1960. (b) Pearson, W. B. *The Crystal Chemistry and Physics of Metals and Alloys*; Wiley-Interscience: New York, 1972.

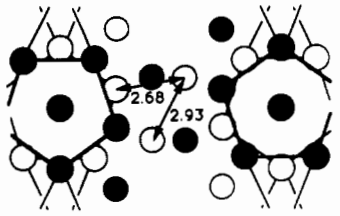

1

shorter than any other in the structure and is quite short when comparison is made with similar metal sulfides.[15] Band structure calculations (discussed further below) yield overlap populations for these close S–S contacts of –0.039, a value that is indicative of significant S–S repulsion. It is interesting to note that the close structural parallels between molybdenum cluster sulfides and selenides is not mirrored by the behavior of reduced tantalum chalcogenides; while the well-known Chevrel phase sulfides and selenides have much in common, the Ta_2S and Ta_2Se structures are quite different.[7] This is perhaps because the close contacts between sulfides in the pentagonal-antiprismatic chain structures (at least Ta_2S and Ta_3S_2) cannot be accommodated by the larger selenides.

Composition of Ta_3S_2. Wada and Onoda reported the phase Ta_3S_{2-x} and determined that it had the same Ta_3S_2 structure, determined by X-ray Rietveld analysis.[4] This Ta_3S_{2-x} phase was reported to exist in the range $0.2 \leq x \leq 0.28$; at the sulfur-rich limit, Ta_3S_{2-x} was said to be accompanied by $2S–Ta_{1+x}S_2$ and at the tantalum-rich limit by Ta_2S.[1] These workers prepared samples by reaction of pressed pellets in alumina crucibles that were sealed in quartz jackets and analyzed by combustion. We were concerned that this procedure could lead to a systematic underestimation of the sulfur content if the samples were subject to oxidation via a transport reaction or reaction with alumina, so we carried out our preparations in sealed Ta capsules. This method carries the risk that the walls of the tube will be involved, but we are able to identify the tantalum sulfides in powder diffraction patterns of analyzed samples and can be fairly certain that inadvertent oxidation has been avoided.

In pellets prepared with the composition $Ta_3S_{2.00}$ and treated as described in the Experimental Section, the Guinier powder diffraction patterns reveal only Ta_3S_2 and a trace of Ta_6S. The absence of Ta_2S suggests that Ta_6S forms at the surface where it is in contact with the surrounding tube and tantalum is locally in excess. (Microprobe analyses of Ta tubes used in tantalum sulfide reactions indicate Ta_6S as the only tantalum sulfide formed.) Combustion analyses of one sample give the composition Ta_3S_x ($x = 1.91 \pm 0.01$). For stoichiometric reactions where the pellet was wrapped with Mo foil, Ta_3S_2 was the only phase detectable in the powder diffraction pattern and the analyzed composition was Ta_3S_x ($x = 2.00 \pm 0.01$).

We attempted the use of an alumina boat to prevent contact with the silica instead of sealed tantalum tubes for the same reaction, and our pellet acquired an uneven whitened coating (thickness $\approx$ 1 mm). This occurred despite a scrupulous flaming of the silica under vacuum prior to sealing. We speculate that remaining traces of H_2O or hydrogen (in the powdered Ta) may serve as transport reagents in these reactions.[11]

The results of reactions run at different compositions are enlightening concerning the phase width of Ta_3S_2 at 1300 °C. In reactions run with a moderate excess (see the Experimental Section) of sulfur, we detect Ta_3S_2 and some $2S–Ta_{1+x}S_2$. On the tantalum-rich side both Ta_2S and Ta_6S are seen in addition to Ta_3S_2, where the Ta_6S is likely formed at the surface (see above). In every case we have evaluated the lattice parameters for the Ta_3S_2 majority phase and find that the parameters show no statistically significant variation as a function of composition. Taken together with the above discussion and the fact that the lattice parameters found in the single-crystal study are little different, we conclude that Ta_3S_2 is essentially a stoichiometric line phase below 1300 °C.

(15) Corbett, J. D. *J. Solid State Chem.* **1981**, *39*, 56.

The possibility of sulfur deficiency in Ta_3S_2 remains as an interesting possibility to contemplate, quite apart from the evidence we have seen that this does not actually occur under the conditions of preparation. Wada and Onoda assumed that substoichiometry in "$Ta_3S_{1.8}$" is accommodated by the occurrence of vacancies in 20% of one of two sulfur positions, though occupancies were not actually varied during their structure refinement. The occurrence of sulfur *vacancies* would appear to be an unlikely prospect since the existence of vacancies implies the loss of four-coordinate sulfur and the creation of Ta centers that are coordinatively unsaturated (see above). This is in contrast to the situation in more dense early-metal sulfides wherein the creation of sulfide vacancies is compensated by a gain in metal–metal bonding surrounding the vacant site. We also note that the sulfur position where Wada and Onoda had assumed 20% vacancies is virtually identical with one of the sulfur positions in Ta_2S, where no indication of vacancies have been reported. Because of the close structural resemblance between the (010) planes of Ta_3S_2 and the (110) planes of Ta_2S, *intergrowth* of these two structures would appear to be a more structurally reasonable way to accommodate variable composition.

Bonding in the Ta_6S_n Series. We now turn to a consideration of the bonding in these structurally remarkable materials. We will present results of band structure calculations for the Ta_2S, Ta_3S_2, and the hypothetical Ta_6S_5 systems and trace the evolution of these systems' electronic structures from bulk bcc Ta metal. To avoid becoming bogged down in too many system-specific details, we will stick to a presentation of the density of states (DOS) plots and the crystal orbital overlap population (COOP) for the Ta–Ta bonds in these systems. A given COOP curve gives us information about the bonding (or antibonding) character of the system's crystal orbitals *with respect to any specific symmetry-unique pair of atoms in the structure.* In other words, one would expect to examine plots for every symmetry-unique bond. In the complex structures we are considering here, we will present curves that are *averaged* over all the short Ta–Ta bonds in the structure, appropriately weighted to reflect the number of each bond type. As we shall see, this provides qualitative information about the metal–metal bonding in these materials without burdening us with too much detailed information.

Before proceeding, some comments on our Ta_6S_5 model chain are in order. We built up the structures of Ta_3S_2 and Ta_2S by using the hypothetical Ta_6S_5 chain as a starting point. This device was suggested by the structural trend that the former *known* tantalum-rich sulfides exhibited. Specifically, we wondered whether the pentagonal-antiprismatic chains present in these compounds might be isolated as distinct one-dimensional entities. We speculate that the form that such one-dimensional chains will take can be surmised by careful inspection of the Ta_3S_2 structure and the ways that it differes from Ta_2S. This led us to focus on the way the additional sulfurs in Ta_3S_2 are accommodated and how the tantalum atoms to which they are bound are structurally affected. It was this process that led us to consider the Ta_6S_5 chain shown in Figure 1. Furthermore, we assume that in any real compound containing these chains that may be synthesized, the environment about the "outer" tantalums will be similar to the Ta2 centers in Ta_3S_2. This means that each of these metals will be bound to the three sulfurs that cap alternant triangular faces of the chain in which the metal in question resides *and* will also be bound to one "ausser" sulfur that fills the last vacant coordination site. Thus, we envision the chains formulated as $^1_\infty[Ta_5TaS_5{}^iS_5{}^a]$ systems where the ausser sulfurs may originate from neighboring chains or perhaps be replaceable by other donor ligands. The structural model used for calculations is shown in Figure 5, where the chain differs from that in Figure 1 only by the addition of ausser sulfides. In the DOS plots for this system, the contribution from these atoms has been subtracted to avoid the appearance of a spurious sulfur "lone-pair peak" at the bottom end of the plotted energy range.

Plots for the total DOS for Ta, Ta_2S, Ta_3S_2, and Ta_6S_5 are shown in Figure 6. In each case the range of energy is restricted so as to capture the Ta d-band region; the sulfur 3s and 3p bands lie lower in energy. For every panel of Figure 6, the shaded levels

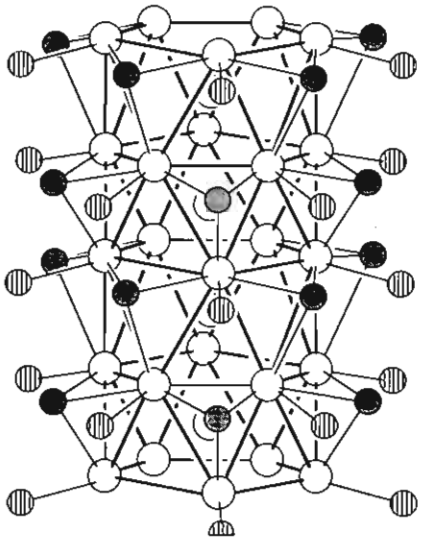

Figure 5. The Ta_6S_5 model chain, complete with ausser sulfides shown as striped balls and placed so as to approximate the environment about Ta2 (see Table II) in Ta_2S_2.

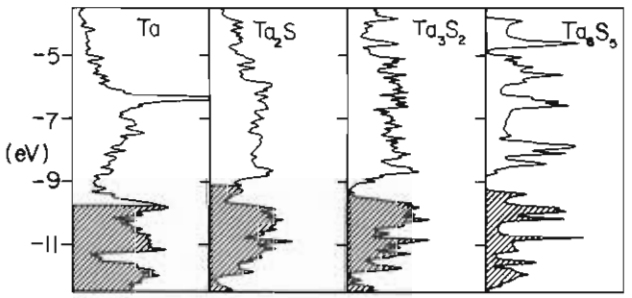

Figure 6. Density of states (DOS) plots for elemental Ta, Ta_2S, Ta_3S_2, and our model $(Ta_6S_5)S_5$ chain. Shaded regions represent the occupied levels in each case. The energy range shows principally the Ta d-band region; the sulfur 3p bands overlap the Ta bands to some extent in lower parts of the range plotted. Note the systematic deepening of the minimum near the Fermi level with increasing sulfur content.

are occupied—the Fermi level chosen for the Ta_6S_5 chain is discussed below. The most important trend observed in these plots is the steady opening of a gap at the Fermi level as the sulfur content increases. There is a local minimum near the Fermi level for Ta_2S, a very deep minimum in Ta_3S_2, and a clear-cut band gap in Ta_6S_5. This sort of behavior seems to be a common characteristic of systems in which the dimensionality of the metal–metal bonded network is reduced. It is also a reasonable hallmark of stable systems that the bulk of the occupied levels are stabilized while unoccupied levels are destabilized. From the molecular point of view this is the expected behavior as well; significant HOMO–LUMO gaps are a very useful qualitative guide to molecular stability.

COOP curves for these systems are no less enlightening. In Figure 7 we show averaged Ta–Ta COOP curves for the same four systems; the energy axes are horizontal and occupied levels are shaded. Each of the sulfides are striking in the extent to which they optimize metal–metal bonding; for each case the Fermi level marks the dividing line between bonding and antibonding levels. This occurs despite the fact that the number of electrons available for metal–metal bonding steadily declines with increasing sulfur content. Apparently, the number of metal–metal bonds lost as tantalum metal is effectively "broken up" by sulfur inclusion is exquisitely in tune with this declining number of available metal–metal bonding electrons.

The calculated electronic structure of these systems clearly suggests the need for further experimentation. We were surprised to see that a small gap (≈0.09 eV) is calculated for Ta_3S_2. Our method of calculation is not of sufficient quantitative reliability for us to be confident of this result, but it does suggest that Ta_3S_2

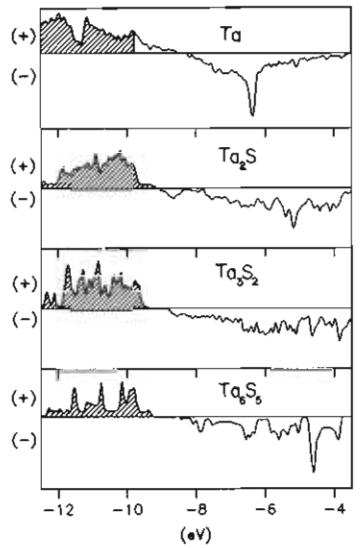

Figure 7. Averaged crystal orbital overlap population (COOP) curves plotted from top to bottom for Ta, Ta_2S, Ta_3S_2, and our model $(Ta_6S_5)S_5$ chain, respectively. The energy range and shading of levels are as in Figure 6.

Table IV. Parameters for EH calculations

	orbital	H_{ij}, eV	$\zeta_1{}^b$	$\zeta_2{}^b$	$c_1{}^a$	$c_2{}^a$
Ta	5d	−9.36	4.76	1.938	0.6105	0.6105
	6s	−8.64	2.28			
	6p	−4.75	2.24			
S	3s	−20.0	2.12			
	3p	−13.3	1.83			

[a] Coefficients used in double-ζ expansion. [b] Slater-type orbital exponents.

is likely be be a rather poor conductor or perhaps behave as a small-gap semiconductor. For structural reasons, anisotropy in the electrical conductivity is also to be expected, with concomitant low conductivity along the [010] direction. The significance of our computational results for the hypothetical Ta_6S_5 chain is amplified by considering the strong correlation between metal–metal "COOP optimization" (i.e., optimization of metal–metal bonding) and the discovery of so many new metal-rich compounds in the last 15 years.[16-22] This has been particularly true for compounds with low-dimensional metal–metal bonded arrays. If nature can be coaxed into somehow cross-linking chains with 5-fold rotational symmetry, our calculations indicate that $^1_\infty[Ta_5TaS_5{}^iX_5{}^a]$ systems should be stable when there are 20 metal-based electrons per Ta_6 unit. The calculated band gap for the model Ta_6S_5 chain system is considerably larger (0.43 eV), and if efforts to synthesize compound(s) containing the neutral Ta_6S_5 chain are successful, we fully expect *semiconducting* behavior. While this is a surprising conclusion, since the chain contains an unbroken and undistorted metal–metal bonded thread and there are a nonintegral number of electrons ($3^1/_3$) per Ta, a similar situation is obtained for the chain compound Gd_2Cl_3,[23] where theory[24] and experiment[25,26] are in agreement on the sem-

(16) Hughbanks, T. *Prog. Solid State Chem.* **1989**, *19*, 329.
(17) Chevrel, R. In *Crystal Chemistry and Properties of Materials with Quasi-One-Dimensional Structures*; Rouxel, J., Ed.; Reidel: New York, 1986.
(18) Adolphson, D. G.; Corbett, J. D. *Inorg. Chem.* **1976**, *15*, 1820.
(19) (a) Torardi, C. C.; McCarley, R. E. *Inorg. Chem.* **1985**, *24*, 476. (b) Torardi, C. C.; McCarley, R. E. *J. Am. Chem. Soc.* **1979**, *101*, 1963.
(20) McCarley, R. E. *Polyhedron* **1986**, *5*, 51.
(21) Simon, A. *J. Solid State Chem.* **1985**, *57*, 2.
(22) Simon, A. *Angew. Chem., Int. Ed. Engl.* **1988**, *27*, 160.
(23) Lokken, D. A.; Corbett, J. D. *Inorg. Chem.* **1973**, *12*, 556.
(24) Bullett, D. W. *Inorg. Chem.* **1985**, *24*, 3319.
(25) Bauhofer, W.; Simon, A. *Z. Naturforsch.* **1982**, *A37*, 568.
(26) Ebbinghaus, G.; Simon, A.; Griffith, A. *Z. Naturforsch.* **1982**, *A37*, 564.

iconducting behavior of the compound.

Acknowledgment. We thank the donors of the Petroleum Research Fund, administered by the American Chemical Society, for partial support of this research. We also gratefully acknowledge the support of the National Science Foundation for support through a Presidential Young Investigator Award (Grant DMR-8858151) and the Robert A. Welch Foundation for support through Grant A-1132. We thank Dr. Nancy McGuire and Roberta Peascoe for assistance in structure refinement and Prof. Abraham Clearfield for generous use of his facilities. Lisa Donaghe performed the microprobe analyses.

Appendix

The extended Hückel method was used for all band structure calculations; parameters appear in Table IV. Valence-state ionization energies (H_{ii}'s) for Ta were previously obtained from a charge-iterative calculation on $Ta_9S_6Ni_2$.[27] Other parameters have been cited previously.[28-30] Except for the Ta_6S_5 model calculation, structural parameters were taken from crystallographic data. For Ta_6S_5, geometric parameters were chosen to closely approximate the chain structure imbedded in Ta_3S_2.

Band structure calculations were carried out by using k point meshes as follows: Ta metal, 32 k points (primitive bcc lattice); Ta_2S, 32 k points for the 36-atom orthorhombic cell; Ta_3S_2, 30 k points for the primitive (20-atom) cell; Ta_6S_5, 25 k points for the one-dimensional $(Ta_{12}S_{10})S_{10}$ unit cell. Each of these k point meshes refers to the number of points used in the irreducible wedge of the appropriate Brillouin zones. All DOS curves were smoothed with Gaussian functions with a standard half-width of 0.05 eV.

Supplementary Material Available: For Ta_3S_2, a table of anisotropic thermal parameters (1 page); a table of structure factors (7 pages). Ordering information is given on any current masthead page.

(27) Hughbanks, T. Unpublished research.

(28) Basch, H.; Gray, H. B. *Theor. Chim. Acta* **1966**, *4*, 367.
(29) Baranovskii, V. I.; Nikolskii, A. B. *Teor. Eksp. Khim.* **1967**, *3*, 527.
(30) Clementi, E.; Roetti, C. *At. Nucl. Data Tables* **1974**, *14*, 177.

Contribution from the Laboratoire de Chimie Inorganique, URA No. 420, Université de Paris Sud, 91405 Orsay, France, Department of Chemistry, University of Bergen, 5007 Bergen, Norway, and Laboratoire de Chimie des Métaux de Transition, URA No. 419, Université Pierre et Marie Curie, 75232 Paris, France

Structural and Magnetic Versatility of the Mn(II)/$[Cu(X_4obbz)]^{2-}$ System (X_4obbz = Oxamido-*N*,*N*'-bis(3,5-dihalogenobenzoato; X = Cl, Br). Crystal Structures and Magnetic Properties of $MnCu(Cl_4obbz)(H_2O)_5$ and $MnCu(Br_4obbz)(H_2O)_3 \cdot 2.5H_2O$

Keitaro Nakatani,[1a] Jorunn Sletten,[1b] Sabine Halut-Desporte,[1c] Suzanne Jeannin,[1c] Yves Jeannin,[1c] and Olivier Kahn*[,1a]

Received April 23, 1990

The two compounds $MnCu(Cl_4obbz)(H_2O)_5$ (**1**) and $MnCu(Br_4obbz)(H_2O)_3 \cdot 2.5H_2O$ (**2**) have been synthesized. Cl_4obbz stands for oxamido-*N*,*N*'-bis(3,5-dichlorobenzoato) and Br_4obbz for oxamido-*N*,*N*'-bis(3,5-dibromobenzoato). Their crystal structures have been determined. The tetrachloro derivative crystallizes in the monoclinic system, space group $P2_1/n$, with a = 10.351 (4) Å, b = 19.130 (4) Å, c = 11.225 (2) Å, β = 97.82 (2)° with Z = 4 MnCu units. The structure consists of binuclear units with Mn(II) and Cu(II) ions bridged by a carboxylate group (Mn···Cu = 5.195 (1) Å). The bimetallic units are connected through Cu···Cl contacts of 2.930 and 3.422 Å. The configuration around the carboxylate bridge is of the anti–syn type. The tetrabromo derivative crystallizes in the monoclinic system, space group $P2_1/c$ with a = 9.294 (2) Å, b = 17.981 (4) Å, c = 15.021 (2) Å, β = 100.00 (2)°, and Z = 4 MnCu units. The structure consists of alternating bimetallic chains with Mn(II) and Cu(II) ions bridged by oxamide (Mn···Cu = 5.341 (2) Å) and carboxylate (Mn···Cu = 5.394 (2) Å) groups. The chains are connected through Cu···Br contacts of 2.971 Å. The configuration around the carboxylate bridge is again of the anti–syn type. The magnetic properties of both compounds have been investigated in the 2–300 K temperature range. For **1**, the molar magnetic susceptibility χ_M follows the Curie law expected for uncoupled Mn(II) and Cu(II) ions. For **2**, χ_M varies as expected for a Mn(II)–Cu(II) pair with a quintet–septet energy gap equal to $3J = -87.0$ cm^{-1}. This rather strong antiferromagnetic interaction occurs through the oxamide bridge. For both compounds, the interaction through the carboxylate bridge is negligible owing to the anti–syn configuration around this bridge. The EPR spectra reveal long-range interactions not detectable through magnetic susceptibility measurements. The structural and magnetic differences between the two compounds are discussed.

Introduction

Recently, we described a molecular-based compound exhibiting a spontaneous magnetization and an hysteresis loop below T_c = 14 K. Its formula is $MnCu(obbz) \cdot H_2O$ with obbz = oxamido-*N*,*N*'-bis(benzoato).[2,3] This compound was obtained from the reaction of the Mn(II) ion on the Cu(II) precursor $[Cu(obbz)]^{2-}$ schematized below:

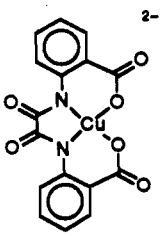

Actually, this reaction, in addition to $MnCu(obbz) \cdot H_2O$, leads to another species of formula $MnCu(obbz) \cdot 5H_2O$, which shows

(1) (a) Université de Paris Sud. (b) University of Bergen. (c) Université Pierre et Marie Curie.
(2) Nakatani, K.; Carriat, J. Y.; Journaux, Y.; Kahn, O.; Lloret, F.; Renard, J. P.; Pei, Y.; Sletten, J.; Verdaguer, M. *J. Am. Chem. Soc.* **1989**, *111*, 5739.
(3) Kahn, O.; Pei, Y.; Nakatani, K.; Journaux, Y. *Mol. Cryst. Liq. Cryst.* **1989**, *176*, 481.

0020-1669/91/1330-0164$02.50/0